INTERNATIONAL JOURNAL OF COMPUTERS COMMUNICATIONS & CONTROL
Online ISSN 1841-9844, ISSN-L 1841-9836, Volume: 19, Issue: 1, Month: February, Year: 2024
Article Number: 4676, https://doi.org/10.15837/ijccc.2024.1.4676

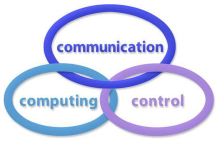

CCC Publications

Neural ordinary differential grey algorithm to forecasting MEVW systems

Zy Chen, Yahui Meng, Ruei-Yuan Wang, Timothy Chen

Zy Chen
School of Science, Guangdong University of Petrochemical Technology, Maoming City, Guan-Du Avenue 525000, No. 139, Peoples R China

Yahui Meng
School of Science, Guangdong University of Petrochemical Technology, Maoming City, Guan-Du Avenue 525000, No. 139, Peoples R China
Corresponding author: mengyahui@gdupt.edu.cn

Ruei-Yuan Wang
School of Science, Guangdong University of Petrochemical Technology, Maoming City, Guan-Du Avenue 525000, No. 139, Peoples R China

Timothy Chen
Caltech, CA 91125, USA
Corresponding author: t13929751005@gmail

Abstract

Because of the advantage of the gray theory for forecasting small sample time data, gray algorithm theory has definitely been extensively utilized since it has been proposed and is currently being widely developed for predicting frames particularly in small sample problems. This article presented a viewpoint called gray algorithm by neuron- based ordinary-differential equation (NODE), called NODGM (neuron-based ordinary-differential gray-mode). In this type, we learn prediction methods through a training process that includes whiting equations. Compared with other models, the structure and time series via the regularity of real-samples are required in advance, so this NODGM design can have a better feasibility of applications and also study the origins of data according to different samples. The purpose is obtaining a better design with high forecast effectiveness, this study uses NODGM to train the model, while Runge-Kutta method is used to have the forecast set and solve numerical framwork. This algorithmic design creates a favorable theoretical basis for the installation of new process and distributes the numerical dimensions of completely mechanically elastic vehicle wheels (MEVW) in practical simulations.

Keywords: fuzzy AI, evolved based controller, Grey DGM (2,1) and algorithm, MEVW, Nonlinear neural network gray.

1 Introduction

Today, energy and resource have become an irreplaceable factor in the economic development of various countries, and all human productive activities require them. Even if there is no urgent need to produce new ones, when used blindly it will consume some of the existing energy. Therefore, for developing a useful academic method that has a magnificent impact on a country's financial development, supplying and production is a direction for the goal.

Currently, there are many prediction methods that use multiple samples, such as fuzzy theory [1-4], neural system [2-6], and graphics systems sciences [7-8]. By better understanding data patterns, Gray control modelling can decrease the sources of un-certainty in small quantity for samples to somehow for making the prediction of small samples more efficient. That implies gray control modeling method was presented by [9] to overcome simulations involving uncertainty. The fundamental design is the name GM algorithmic model (1.1). The reason of gray theory is effective, fast and cheap, it was externally utilized by researchers for many decades to publish journal papers in different fields, including civil engineering and computer science [4-9]. Because of additional modeling studies (1, 1), all kinds of theorems were emerged [8-9]. These existing foundlings corrected the foundation of such GM(1,1) models , which usually gives us higher accuracy.

When searching for grayscale patterns, many studies will have the similar type of structures, combining it by the viewpoiints of simple patterns, using discrete grayscale patterns to obtain the (1, 1) pattern [10-12] These models produce poor results when the sample data is homogeneous . Based on [10-14] proposed an ND combined GM model that was extended to experimental data [15]. Actual sample documents generally would not achieve uniformity because the GM(1,1) approximation is close to the cube model , which significantly limits its feasibility. NGM(1, 1, k) method [16-18] was presented to address these drawbacks. But, this design illustrates several new methods. The instance by the gray design is actually less powerful than the GM(1,1) model in terms of predicting instantaneous series, although it can achieve higher accuracy in samples with non-uniform exponential properties. Finally, [19-22] provided the ON combined GM design to overcome the simulation in applications. [23-25] integrated different parameters with the fuzzy neural type and alleged a grayscale forecast prototype in point function quoted by [26-27]. Since the kernel method is effective and feasible in different kinds of simulations and experiments, many scholars are glad to adopt the viewpoints of features to propose the modified version of algorithm on the kernel method [28-32]. This method can effectively predict nonlinear series based on these criteria.

The gray differential Eq is a new neural system developed by [32] was proposed in advanced test. A passage is performed successively between modeling neurons of the remaining network [33-37]; Therefore, the whole frameworks are continuous and adaptive using original gray equations. It was attracted by scholars with the earnest and efforts paying attention for a new application and practical tests even a new field of NNs. Therefore, it is commonly adopted in many mechanisms and advanced studies [38-40].

In this article, we found variables were estimated using algorithmic methods such as least squares based on the fading theory. By identifying the DE, the expected process must calculate a good level. However, without proper knowledge there is no guarantee that the defined model terminology and configuration are consistent with the actual material properties. Second, although the gray model is suitable for predicting different sample sizes, its test is reducing empirical least squares variables, that tells forecast is according to larger samples. That is, when using the least squares method under small sample conditions, obesity is more likely to occur. To solve these problems, this paper collaborates with NODE and proposes a novel gray forecast design by defining NODE's fading Eq. Moreover, there is no need to propose obvious configurations and jargons since the optimal model is obtained by a AI process which could be solved using the Runge-Kurth method . We believe that the NODGM model can be used for information with differentials. Since the design is trained according to the slope function, which controls the loss threshold, NODE can be trained to decrease the errors and upgrade the results.

In the rest sections, we give the organization of the article . Section 2 presents the main components of the GM method (1.1). We introduce the theory of NOD combined GM and NO combined DE in Section 3. Section provides one practical simulation in test of fuzzy and neural gray algorithm. Finally,

Section 4 summarizes the research and concludes the findings.

2 Gray model

The innovative models of fundamental genetic modification methods are available (1,1). Currently, this article will introduce the series approximating method and variable estimation method (GM(1,1) method) of this basic model, as shown in Equation (1)

$$\left(x^1(1), x^1(2), x^1(3), \ldots, x^1(n)\right) \tag{1}$$

The sequence is a generated order of stacked queues.

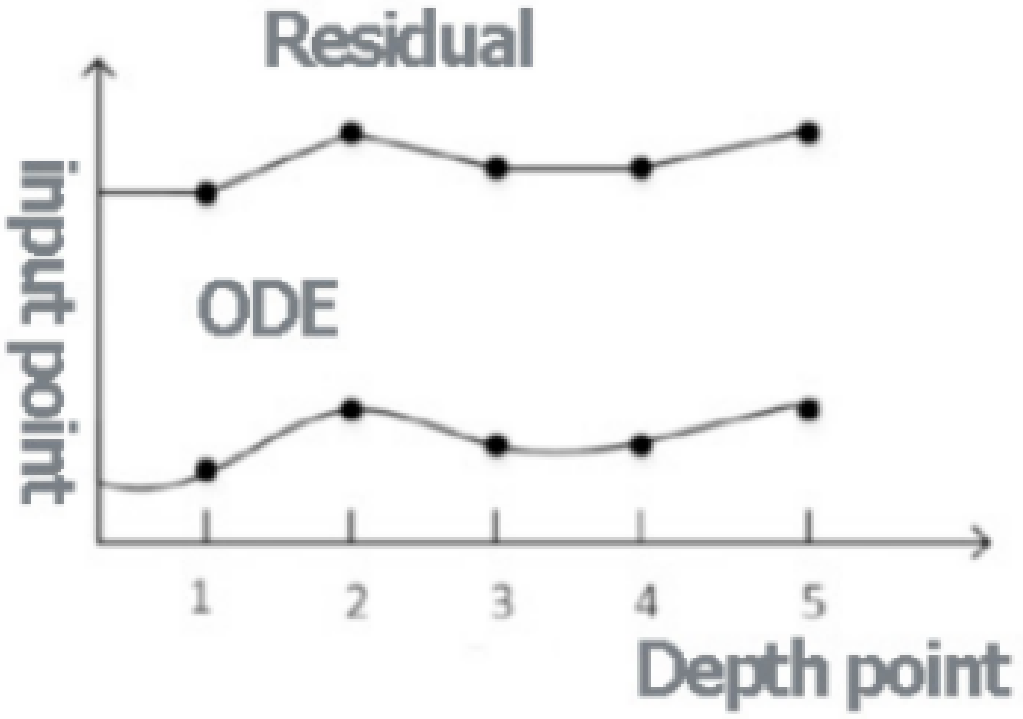

Fig. 1. Transformation differences between residual networks and ODE networks.

$$\left(x^0(1), x^0(2), x^0(3), \ldots, x^0(n)\right) \tag{2}$$

$$x^0(1) + \alpha z^1(t) = b \tag{3}$$

and $x^1(k) = \sum_{t=1}^{k} x^0(t), z^1(k) = \frac{1}{2}\left(x^1(k-1) + x^1(k)\right)$
When (4) is applied:

$$z^1 = \left(z^1(2), z^1(3), z^1(4), \ldots, z^1(n)\right) \tag{4}$$

It is a set of values differential equation

$$\frac{dx^1(t)}{dt} = -ax^1(t) + b \tag{5}$$

GM(1,1) is

$$X = [x^0(2), x^0(3), \ldots, x^0(n)]^T, C = \begin{bmatrix} -z^1(2) & 1 \\ -z^1(3) & 1 \\ \vdots & \vdots \\ -z^1(n) & 1 \end{bmatrix}, Y = [a, b]^T$$

These vectors of the form (3) can be defined

$$X = CY \tag{6}$$

If we remove parameter values and numerical coefficients from the equation, then

$$Y = C^T \left(C^T C\right)^{-1} X \tag{7}$$

Put e the numerical coefficient in equation (5) and we solved it to get this solution as below.

$$\hat{x}^1(t) = \frac{b}{a} + \left(x^0(1) - \frac{b}{a}\right) e^{-a(t-1)} \tag{8}$$

These predictions from source data are captured with $\hat{x}^0(t)$:

$$\hat{x}(t) = -\hat{x}(t-1) + \hat{x}(t), t = 2, 3, \ldots, n \tag{9}$$

3 Methodology of NODGM

Before presenting the method, neuron-based ordinary differential equations are described in Section 3.1 below.

3.1 A N.O.D.E. (Neural-based ordinary-differential equation)

The neural constant differential equation is characterized by a unique NN. This is shown in Figure 1 , where the rest of each layer of the network has its own transformation function f (h(t), θ(t)); Therefore, the whole network expresses the neural network. A range of different driveway layouts . However, curve h(t) represents a harmonic curve, as shown in the last row of Figure 1, showing that the NN could use equations with original differentials (ODE).

For such continuous neural networks, this study uses a general NN approximating method to gain differential inclusions. First solve the ordinary differential equation. For each t the value of the value h(t) can be calculated.

NODE c can in fact be regarded as a specific residual concept of network. The framework is the row of remaining diagrams, showing in Fig. 2 . Regarding the NN criterion, each block in the ODE NN has the same transformation function f. In Fig. 2 this describes the remaining block, which represents the input h(t) and the output h(t+1), and obtain:

$$h(t+1) = h(t) + f\left(h(t), \theta_t\right) \tag{10}$$

$$h(t+1) = h(t) + kf(h(t), \theta, t) \tag{11}$$

$$\frac{dh(t)}{dt} = f(\theta, t, h(t)) \tag{12}$$

Among them, k is step size and k have the given number 1. When the variable t is 0, Eq (12) becomes equation (10). Eq (12) means solution is unique and balanced, because there is one real solution .

The state of the NODE represents all the data that can be generated. Like simple neural systems, NODE training must follow the necessary backscatter transmission. Recently, several advanced modeling has been made available to solve ODEs. For example, the Runge-Kutta approximation [41-47] is a general ODE solution and its accuracy is higher than the Euler approximation. For the description in the ODE method

$$y\left(x_0\right)=y_0, y'=f(x,y), x\in[x_0,x_f] \tag{13}$$

We have

$$y_{n+1}=y_n+\frac{s}{6}\left(K_1+2K_2+2K_3+K_4\right) \tag{14}$$

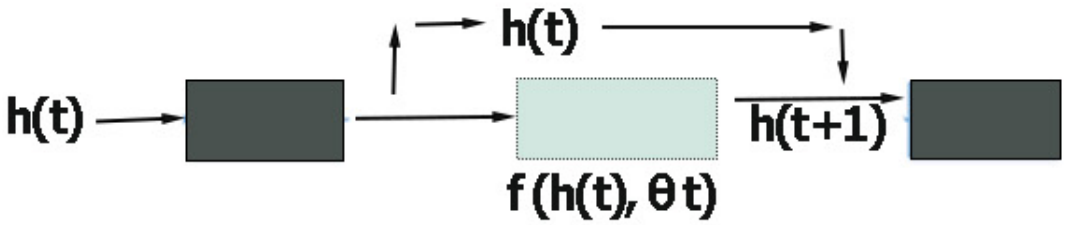

Fig. 2. The process of generation of computation

Eq. (14) is the iteration height value and has a fixed step size, making it more complicated than the adjustable size-step method [48-55].

Therefore, this study can describe ODEsolver as the redirector;

$$\begin{aligned} h(t) &= h\left(t_0\right)+\int_{t0}^{t} f(h(t),\theta,t)dt \\ &= \text{ ODESolver } \left(h(t),h\left(t_0\right),t,f((h(t),\theta,t),\theta)\right) \end{aligned} \tag{15}$$

$$L=\left(ODESolver\left(h\left(t_0\right),\theta,t,t_0\right)-S\right)^2 \tag{16}$$

$$\frac{da(t)}{dt}=-a(t)^T\frac{\partial f(h(t)\theta,t)}{\partial h} \tag{17}$$

ODESolver obtains the response based on the initial values θ,h (0), the initial value t_0 and the final t with ODE response in Eq (1). When using ODESsolver, the equation (11) would be obtained. Pass equations on nodes. (15), we can obtain h(t). Thus, according to f((h(t), θ, t)), we could easily obtain the f that is related to the computational range of the h. By telling ODESolver to calculate (h(t0, t0, θ, t), the final position a(tn) = ∂L can be calculated directly. Then the ODE solver can solve equation (17) and count all end state a(tn).

$$a(t)=ODESolver\left(a\left(t_n\right),t,\frac{\partial f((\ \mathrm{h(t)},\theta,\mathrm{t})}{\partial h}\right) \tag{18}$$

To $a(t)$ obtain the score, the parameter $\frac{\partial L}{\partial \theta}$ must be determined.

$$\frac{dL}{d\theta}=\int_{t1}^{t0} a(t)^T\frac{\partial f(t,\theta,h(t))}{\partial\theta}dt \tag{19}$$

Finally, we can have this slope for setting variables and perform the recovery process.

3.2 ODGM neural reasoning

In this part, the algorithm proposes a new gray design. Considering the conditions f(t) and $x_1(t)$, the θ is in the NODGM model. Then

$$f\left(x^1(t),t,\theta\right)=\theta_1 g_1\left(x^1(t),t\right)+\theta_2 g_2\left(x^1(t),t\right)+\cdots+\theta_n g_n\left(x^1(t),t\right) \tag{20}$$

where is $f\left(x^1(t),t,\theta\right)t$ which $x^1(t)$ is a series of analogous transformations. A DNN was thought of as a replaces between its inputs. Given an input, estimate $x^1(t)$ the function from which the DNN can be obtained f. In view of this, $h(t)=x^1(t)$ the fading rules of the NODGM numerical approach can be obtained as numerical periods;

$$f(\ \mathrm{h(t)},\theta,\mathrm{t})=\frac{dh(t)}{dt} \tag{21}$$

is defined θ and f is the value of the weight. When we f fit a NN to obtain a number (t), the model can have different modes, for example: Uneven Uniform, non-linear or Linear. Given the sum of $tspan$ the initial value terms θ ODESsolver can then be $h(0)$ used to obtain the prediction method H.

$$H=ODESolver(h(t),t,f(\ \mathrm{h(t)},\theta,\mathrm{t}),h(0),\ \mathrm{spant}\ ,\theta)=[h(0),\hat{h}(0+1),\ldots,\hat{h}(0+n-1)] \tag{22}$$

We assume capabilities to manage digital NODs Optimization parameter θ.

$$L=\left\|H-X^0\right\|_2^2=\sum^{\mathrm{n}}(\hat{h}(t)-h(t))^2 \tag{23}$$

Thus, the design is according to parameterized slopes instead of the least squares method. Since this fading function is obtained from NN, the above data is recorded in the raster method at the same time, which greatly decreases the time consumption to use ODE.

If there exists a both positive and definite symmetric matrix $P(x)$, the control gain $\mathrm{K_i(y)}\in \mathrm{R^{m\times q}}$ and a scalar $\gamma>0$ satisfy the following inequalities

$$\delta\mathrm{x}=\mathrm{A}_\mu(\mathrm{x})\mathrm{x(t)}+\mathrm{B}_\mu(\mathrm{x})\mathrm{z(t)u(t)}=\mathrm{C}_{1\mu}(\mathrm{x})\mathrm{x(t)}+\mathrm{D}_\mu(\mathrm{x})\mathrm{u(t)y(t)}=\mathrm{C}_{2\mu}\mathrm{x(t)} \tag{24}$$

Then the discrete-fuzzy closed-loop system (2.6) can be stabilized and satisfied with the static output feedback controller $\|\mathrm{H(s)}\|_\infty<\gamma$.

For the comprehensive analysis of the static output feedback controller, we use Lyapunov's theorem to analyze its stability, where the Lyapunov function $V(x)$ is expressed as the following form

$$\mathrm{V(x)}=\mathrm{x^T(t)x(t)P^{-1}(x)} \tag{25}$$

Now $0>\Delta\mathrm{V(x)}-\gamma^2\omega^{\mathrm{T}}\omega+\mathrm{z^Tz}$, where $\Delta\mathrm{V(x)}=\mathrm{V(x(td+1))}-\mathrm{V(x(td))}$, while $\mathrm{V(x(td+1))}=\mathrm{x^T(td+1)P^{-1}\left(x^+\right)x(td+1)}$, $\mathrm{x^+}$ means $\mathrm{x(td+1)}$, then

$$\begin{aligned}
&=\mathrm{x^T(t+1)P^{-1}\left(x^+\right)x(t+1)-x^T(t)P^{-1}(x)x(t)-\gamma^2\omega^T\omega+z^TZ}\\
0>\Delta\mathrm{V(x)}-\gamma^2\omega^{\mathrm{T}}\omega+\mathrm{z^Tz}&=\begin{bmatrix}\mathrm{x}\\ \omega\\ \mathrm{T}\end{bmatrix}^{\mathrm{T}}\begin{bmatrix}\mathrm{A}^{\mathrm{T}}_{\mu\mu\mu}(\mathrm{x,y})\mathrm{P^{-1}\left(x^+\right)}\star-\mathrm{P^{-1}(x)}+\mathrm{C}^{\mathrm{T}}_{\mu\mu\mu}(\mathrm{x,y})\mathrm{C}_{\mu\mu\mu}(\mathrm{x,y}) & A^{\mathrm{T}}_{\mu\mu\mu}(x,y)P^{-1}\left(x^+\right)B_{\infty\mu}(x)+C^T_{\mu\mu\mu}(x,y)D_{\infty\mu}(x)\\ -\mathrm{B}^{\mathrm{T}}_{\infty\mu}(\mathrm{x})\mathrm{P^{-1}\left(x^+\right)A}_{\mu\mu\mu}(\mathrm{x,y})+\mathrm{D}^{\mathrm{T}}_{\infty\mu}(\mathrm{x})\mathrm{C}_{\mu\mu\mu}(\mathrm{x,y}) & B^T_{\infty\mu}(x)P^{-1}\left(x^+\right)B_{\infty\mu}(x)+D^T_{\infty\mu}(x)D_{\infty\mu}(x)-\gamma^2I\end{bmatrix}\begin{bmatrix}x\\ \omega\end{bmatrix}
\end{aligned} \tag{26}$$

which $A^{\mathrm{T}}_{\mu\mu\mu}(\mathrm{x,y})\mathrm{P^{-1}\left(x^+\right)}\star$ means $\mathrm{A}^{\mathrm{T}}_{\mu\mu\mu}(\mathrm{x,y})\mathrm{P^{-1}\left(x^+\right)A}_{\mu\mu\mu}(\mathrm{x,y})$ that the above formula means equation $-(G(x)-P(x))^TP^{-1}(x)(G(x)-P(x))\le 0, P(x)>0$ after expanding the transposition, we get $-\mathrm{G^T(x)P^{-1}(x)G(x)}\le-\mathrm{G(x)}-\mathrm{G^T(x)}+\mathrm{P(x)}$.

Therefore can be rewritten as the following formula

$0>\sum^{\mathrm{r}}_{\mathrm{i}=1}\sum^{\mathrm{r}}_{\mathrm{j}=1}\sum^{\mathrm{r}}_{\mathrm{k}=1}\mu_{\mathrm{i}}\mu_{\mathrm{j}}\mu_{\mathrm{k}}\chi_{\mathrm{ijk}}(\mathrm{x,y})$

4 Case study

The gray mode (2.1) will assure that practical simulations are coherent and adaptive. The design unit utilize to the Oracle gray signal and has an adaptive power control that can observe the movement with an advanced control design, which is very suitable for stabilizing the response of MEVW.

To verify the control scheme, the appropriate first step is DGM (2.1). Using the a practical example to demonstrate a motion digital control design, the assumed condition would be from and to within seconds, thus a Simulink phase was designed to approximate the real cases of vibrations (pulse: and phase) to capture the performance of demonstration by analysis. This demonstration, acting MEVW, represents a fixed delay corresponding to the state, velocity and rhythm of acceleration by the vehicle. The certain simulator factors are summarized in Table 1.

This experiment of demonstration can be seen in Figure 3 depicting the predictions of the GDM (2.1) design and the accurate input is very small, especially when the evolution is relatively less. It is still suitable for engineering demonstrations. Therefore, reliable properties can also be specified in DGM (2.1). The matrix weights in the group layer and feedbacks are represented by and once trained with the Back Propagation network, this weighting values can be recorded. There are comparisons and approximation in Eq. (24).

$$\begin{aligned} &v_r^1 = W_{1r}^1 x(k) + W_{2r}^1 x(k-1) + W_{3r}^1 u(k), \\ &v_1^2 = W_{11}^2 T\left(v_1^1\right) + W_{21}^2 T\left(v_2^1\right) + W_{31}^2 T\left(v_3^1\right), x(1+k) = T\left(v_1^2\right) \end{aligned}$$

$$x(1+k) = \left(h_{11}^2(k) g_1 + h_{12}^2(k) g_2\right) v_1^2 = \sum_{i=1}^{2} h_{1i}^2(k) g_i v_1^2 \tag{27}$$

Moreover, the NN design is according to the matrix number in the lunear differtial inclusion command, as shown below.

$$x(k+1) = \sum_{i=1}^{16} h_i(k) \left\{B_i u(k) + A_i x(k)\right\} \tag{28}$$

and

$$\begin{aligned} A_1 = A_2 = \cdots = A_9 = \begin{bmatrix} 0 & 0 \\ 1 & 0 \end{bmatrix}, A_{10} = \begin{bmatrix} -0.0598 & -0.2443 \\ 1 & 0 \end{bmatrix}, \\ A_{11} = \begin{bmatrix} 0.0148 & -0.0214 \\ 1 & 0 \end{bmatrix}, B_{12} = \begin{bmatrix} -0.0120 \\ 0 \end{bmatrix} - A_{14} = \begin{bmatrix} 0.0668 & -0.2482 \\ 1 & 0 \end{bmatrix} \\ A_{12} = \begin{bmatrix} 0.1266 & -0.0039 \\ 1 & 0 \end{bmatrix}, A_{13} = \begin{bmatrix} -0.0451 & -0.2657 \\ 1 & 0 \end{bmatrix}, \\ A_{15} = \begin{bmatrix} 0.1414 & -0.0252 \\ 1 & 0 \end{bmatrix}, A_{16} = \begin{bmatrix} 0.0816 & -1.2695 \\ 1 & 0 \end{bmatrix}, \\ B_1 = B_2 = \cdots = B_9 = \begin{bmatrix} 0 \\ 0 \end{bmatrix}, B_{10} = \begin{bmatrix} -0.1172 \\ 0 \end{bmatrix}, B_{11} = \begin{bmatrix} 0.0266 \\ 0 \end{bmatrix}, \\ B_{13} = \begin{bmatrix} -0.0906 \\ 0 \end{bmatrix}, B_{14} = \begin{bmatrix} -0.1292 \\ 0 \end{bmatrix}, B_{15} = \begin{bmatrix} 0.0147 \\ 0 \end{bmatrix}, B_{16} = \begin{bmatrix} -0.1025 \\ 0 \end{bmatrix}. \end{aligned} \tag{29}$$

The height curve is shown in Fig. 4(a). Observing 0.9 second, the amplitude of the next signal step is 0.11 m, so the height of this path is assumed to be fixed. In the observation, a suspension design of the active matrix in MEVW would be applied. Thus, Figure 4(b) shows a visualization of the input of objects during a one-second towing time. The optimal steering control of the actuators is 11,460 N, while the steering force of the rear suspension drops to 13,690 N in 0.4 seconds after 25 minutes. The vehicle stabilizes for some time without steering intervention. Figures 4(c) and 4(d) show the up and down states including displacements and movements takeoff. Overtaking with or without a gray signal may: Cause intentional but uncontrolled case ($>$ 3.5 seconds). This may make the car more stable

(e.g. <2.5 seconds). Although adaptive power control by proposed forecast is better than traditional habit prediction, the amount of up and down movement is bounded by as much as 7.64%, and the upward movement is also suppressed. About 18% and 7.5%. When grayscale signal prediction is used, the error is expected more than when grayscale signal forecast is not used.

Table 1: some measurable design algorithmic factors.

characteristics	variables	Unites	tests	varaibles	Unites
19,630	A021	N*m1	728	M	kg
1	A022	N*m2	1232	Iy	kg*m2
1	A023	N*m3	42	m1	kg
1296	B021	N*s*m1	42	m2	kg
1	B022	N*s2*m2	9.81	g	m*s2
1	B023	N*s3*m3	1.21	a	m
0.001	d	M	1.8	b	m
3000	Csky01	N*s*m1	10	v	m*s1
3000	Csky02	N*s*m1	176,220	A011	N*m1

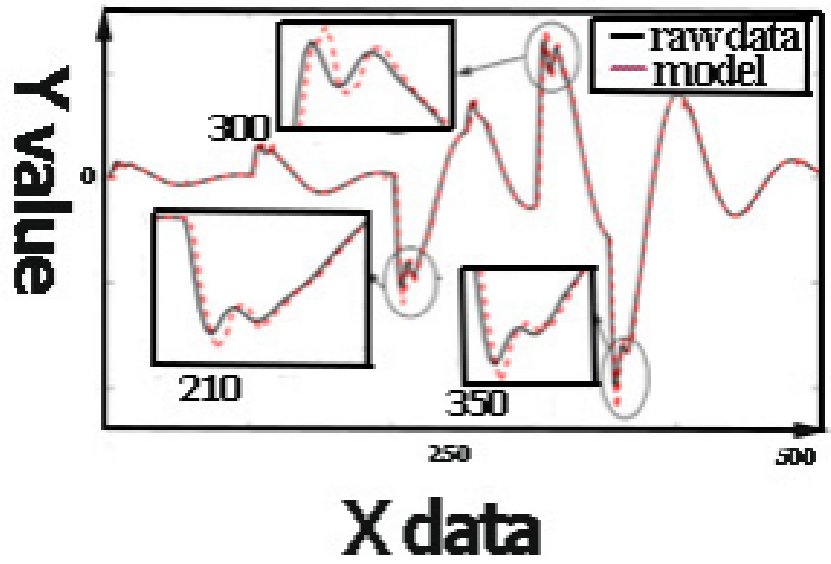

Fig. 3. Comparison of random numerical data and predictions of the DGM(2,1) model.

Figures 4(e) and 4(f) show the vertical movement of all wheels by fuzzy neural control with gray algorithm. As shown in the figure, the maximum limitation of front wheel movement without steering is 0.23 meters, while in normal mode, the maximum limitation of front wheel movement per revolution is 0.17 meters. 0.13 m, and the up and down vibration of the back was reduced by 0.037 m; the opposite conditioned stimuli happens in proposed test. The wheel allows for smooth adjustment, which stabilizes the body and ensures stable driving of the car. Overall this demonstration is believed suitable when the data is projected in grayscale.

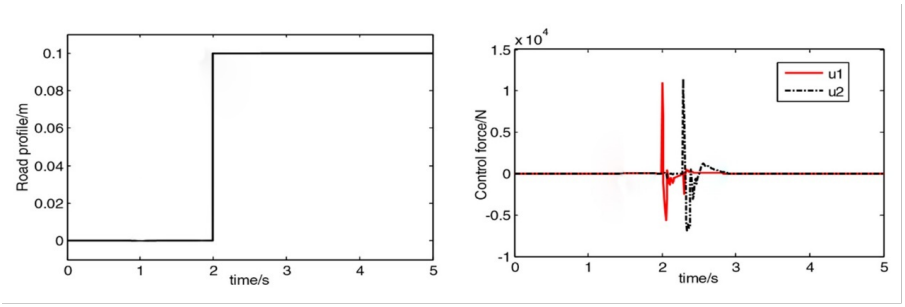

(a) test profile in progress (b) Sign inspection

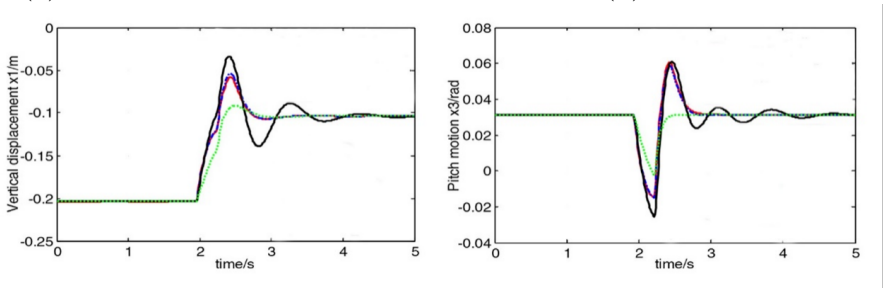

(c)Movement of vibrationV from the vertical car(d) Movement of vibrationV from the car to the track

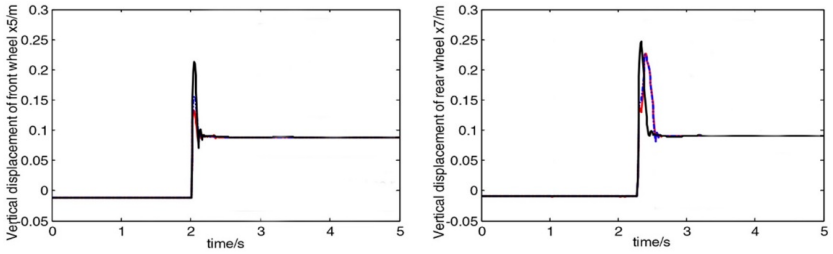

(e) Vibration V moves vertically from the front wheel. (f) V-vibration motion of the rear wheel

Fig. 4. Comparisons with delay consideration in vibration response with controller.

Fig. 5 is the whole computer simulation process for observation in trajectory diagram. Firstly, the nonlinear term $sin(x_1)$ in the global interval $\in [-\infty, \infty]x_1$ is fuzzified by fuzzy technique , and a polynomial model is established to facilitate subsequent numerical simulations and finally solve the gain to design controller.

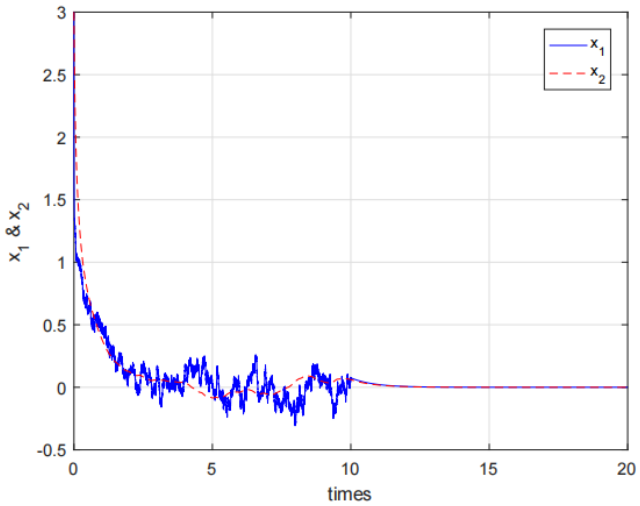

Fig.5. time-domain trajectory diagram

This paper proposed the novel algorithm was adaptive in a practical engineering application. It

integrates a linear differential NN design with Lyapunov method for systems. Based on this knowledge, we will demonstrate it in this paper using the proposed criteria-based $H\infty$verification method. To check its practical usefulness, a practical simulated suspension model was adopted for demonstration. The result indicates that the linear differential gray neural network scheme enhanced with linear Lyapunov have successful control outcomes.

5 Conclusions

This study is based on model NODE, which offers a new gray model. Compared to gray models that manually define concepts and structures, the NODGM model introduces many features and flexible models related to learning different paradigms, which means that NODGM will be widely used. At the same time, these gradients are quite complex compared to least squares, but they cope with iterative losses and prevent obesity. Therefore, NODGM provides a higher generalization result than model of the least squares. These simulation experiments demonstrate that the model NODGM can effectively predict real short-term control conditions of nonlinear systems. Thus, our model could be utilized to predict all applications in practical and is also considered robust in processes of decision-making and engineering systems. However, this model in study still has extra two problems. Firstly, lower initial network weights may result in reduced localization during training and therefore lower model performance. Secondly, some shape changes could be made for reducing the weight and thus increase the model strength. In our current work, the authors plan to improve this proposed model.

Declarations

Data Availability, Funding, Consent for publication and Consent to Participate

Not Applicable.

Compliance with Ethical and Data Availability Statements

The authors declare that they have no conflict of interest with the publication of this article. All analyzed data and measurements are included in the article not only for illustration purposes, but also as examples within this study. The application of the methods in this article is original and has not been submitted for publication in other journals.

Acknowledgments

The authors are grateful for the research grants of GDUPT, Peoples R China under Grant NO. 2019rc098, and the Grant NO. NO. 2021rc002 in Guangdong Province, Peoples R China. Also, the authors wish to appreciate to constructive suggestions from the anonymous reviewers. Professor Chen conducted a comprehensive review of the literature on the above topics and contributed to the revision of this article. He also writes reviews and comparisons of various algorithmic techniques and artificial intelligence methods. The first version of this manuscript was written by Dr. Chen and all authors commented and contributed to revisions of the manuscript. The final manuscript was read and approved by all authors. Doctor. Jiang also participated in this work and presented the work of Dr. Meng confirms that the literature review presented is sufficiently relevant and informative for readers of peer-reviewed journals. Additionally, Professor Wang's extensive knowledge of various control technologies provides insightful and easy-to-understand explanations. Professor Timothy participated in discussions on several nonlinear mechanical architectures. His technical background allows him to find functional designs that meet the highest demands of our times. Finally, Dr. Meng, who designed an algorithm characterized by high convergence speed, simple parameter setting and memory capacity. Therefore, the gray neural network learns the path of the wolves, randomly generates initial values in the solution space to simulate the positions of the wolves, and uses contours and attack patterns to approximate the optimal solution. The improved linear differential gray neural network scheme algorithm changes the convergence speed to increase the global search speed, avoid falling into the best solution in the field, increase memory capacity, improve convergence performance, add

weights to more features and research notes add and create. It is simpler and uses selfish strategies to avoid unnecessary searches. NODGM combines a linear differential neural network scheme with the Lyapunov stabilization method for nonlinear suspension systems.

References

[1] G. Zhou, R. Zhang, and S. Huang, Generalized Buffering Algorithm IEEE access, 9, 27140-27157. doi: 10.1109/ACCESS.2021.3057719, 2021

[2] Z. Luo, H. Wang and S. Li Prediction of International Roughness Index Based on Stacking Fusion Model *Sustainability*, vol. 14(12), pp. 6949. https://doi.org/10.3390/su14126949, 2022.

[3] Z. Lin, H. Wang, and S. Li Pavement anomaly detection based on transformer and self-supervised learning *Automation in Construction*, [3]vol. 143, pp. 104544. doi: https://doi.org/10.1016/j.autcon.2022.104544, 2022.

[4] Q. She, R. Hu, J. Xu, M. Liu, K. Xu, and H. Huang. Learning High-DOF Reaching-and-Grasping via Dynamic Representation of Gripper-Object Interaction *ACM Trans. Graph*, vol. 41(4), doi: 10.1145/3528223.3530091, 2022.

[5] Q. Ni, J. Guo, W. Wu, H. Wang, and J. Wu Continuous Influence-Based Community Partition for Social Networks *IEEE Transactions on Network Science and Engineering*, [5]vol. 9(3), pp. 1187-1197. doi: 10.1109/TNSE.2021.3137353, 2022.

[6] D. Li, H. Yu, K.P. Tee, Y. Wu, S. S. Ge, and T. H. Lee On Time-Synchronized Stability and Control *IEEE TRANSACTIONS ON SYSTEMS MAN CYBERNETICS-SYSTEMS*, [6]vol. 12, pp. 1-14. doi: 10.1109/TSMC.2021.3050183, 2021.

[7] H. Yuan, and B. Yang System Dynamics Approach for Evaluating the Interconnection Performance of Cross-Border Transport Infrastructure *JOURNAL OF MANAGEMENT IN ENGINEERING*, vol. 38(3), doi: 10.1061/(ASCE)ME.1943-5479.0001015, 2022.

[8] S. Jiang, C. Zhao, Y. Zhu, C. Wang, Y. Du, W. Lei, and L. Wang A Practical and Economical Ultra-wideband Base Station Placement Approach for Indoor Autonomous Driving Systems *Journal of advanced transportation*, doi: 10.1155/2022/3815306, 2022.

[9] J. Xu The Alleviation of Perceptual Blindness During Driving in Urban Areas Guided by Saccades Recommendation *IEEE Transactions on Intelligent Transportation Systems*, doi: 10.1109/TITS.2022.3149994, 2022.

[10] J. Xu The Improvement of Road Driving Safety Guided by Visual Inattentional Blindness *IEEE Transactions on Intelligent Transportation Systems*, vol. 23(6), pp. 4972-4981. doi: 10.1109/TITS.2020.3044927, 2022

[11] W. Zhang, Z. Zheng, and H. Liu Droop control method to achieve maximum power output of photovoltaic for parallel inverter system *CSEE Journal of Power and Energy Systems*, [11]vol. 8(6), pp. 1636-1645. doi: 10.17775/CSEEJPES.2020.05070, 2022.

[12] K. Xu, Y. Guo, Y. Liu, X. Deng, Q. Chen, and Z. Ma 60-GHz Compact Dual-Mode On-Chip Bandpass Filter Using GaAs Technology *IEEE Electron Device Letters*, [12]vol. 42(8), pp. 1120-1123. doi: 10.1109/LED.2021.3091277, 2021.

[13] J. Xu, K. Guo, and P. Z. H. Sun Driving Performance Under Violations of Traffic Rules: Novice Vs. Experienced Drivers *IEEE Transactions on Intelligent Vehicles*, [13]doi: 10.1109/TIV.2022.3200592, 2022.

[14] Z. Wu, J. Cao, Y. Wang, Y. Wang, L. Zhang, and J. Wu hPSD: A Hybrid PU-Learning-Based Spammer Detection Model for Product Reviews *IEEE transactions on cybernetics*, vol. 50(4), pp. 1595-1606. doi: 10.1109/TCYB.2018.2877161, 2020

[15] N. Huang, Q. Chen, G. Cai, D. Xu, L. Zhang, and W. Zhao Fault Diagnosis of Bearing in Wind Turbine Gearbox Under Actual Operating Conditions Driven by Limited Data With Noise Labels *IEEE Transactions on Instrumentation and Measurement*, vol. 70, pp. 1-10. doi: 10.1109/TIM.2020.3025396, 2021.

[16] S. Lu, Y. Ding, M. Liu, Z. Yin, L. Yin, and W. Zheng Multiscale Feature Extraction and Fusion of Image and Text in VQA *International Journal of Computational Intelligence Systems*, vol. 16(1), pp. 54-58. doi: 10.1007/s44196-023-00233-6, 2023.

[17] J. Song, A. Mingotti, J. Zhang, L. Peretto, and H. Wen Accurate Damping Factor and Frequency Estimation for Damped Real-Valued Sinusoidal Signals *IEEE Transactions on Instrumentation and Measurement*, vol. 71. doi: 10.1109/TIM.2022.3220300, 2022.

[18] X. Liu, G. Zhou, M. Kong, Z. Yin, X. Li, L. Yin, and W. Zheng Developing Multi-Labelled Corpus of Twitter Short Texts: A Semi-Automatic Method *Systems*, vol. 11(8), pp. 390-398. doi: 10.3390/systems11080390, 2023.

[19] X. Zhang, W. Pan, R. Scattolini, S. Yu, and X. Xu Robust tube-based model predictive control with Koopman operators *Automatica*, 64(5), 2122-2127. doi: 10.1109/TAC.2018.2872197

[20] X. Zhang, S. Wen, L. Yan, J. Feng, and Y. Xia A Hybrid-Convolution Spatial–Temporal Recurrent Network For Traffic Flow Prediction *The Computer Journal*, vol. c171. doi: 10.1093/comjnl/bxac171, 2022.

[21] Y. Xiao, Y. Zhang, I. Kaku, R. Kang, and X. Pan Electric vehicle routing problem: A systematic review and a new comprehensive model with nonlinear energy recharging and consumption *Renewable and Sustainable Energy Reviews*, vol. 151, 111567. doi: https://doi.org/10.1016/j.rser.2021.111567, 2021.

[22] M. Yang, Y. Wang, C. Wang, Y. Liang, S. Yang„ Wang, L.S. Wang Digital twin-driven industrialization development of underwater gliders *IEEE Transactions on Industrial Informatics*, doi: 10.1109/TII.2023.3233972, 2023.

[23] X. Bai, Y. He, and M. Xu Low-Thrust Reconfiguration Strategy and Optimization for Formation Flying Using Jordan Normal Form *IEEE Transactions on Aerospace and Electronic Systems*, vol. 57(5), pp. 3279-3295. doi: 10.1109/TAES.2021.3074204, 2021.

[24] H. Wang, X. Zhang, and S. Jiang A Laboratory and Field Universal Estimation Method for Tire–Pavement Interaction Noise (TPIN) Based on 3D Image Technology *Sustainability*, vol. 14(19). doi: 10.3390/su141912066, 2022.

[25] Q. Li, H. Lin, X. Tan, and S. Du H∞ Consensus for Multiagent-Based Supply Chain Systems Under Switching Topology and Uncertain Demands *IEEE Transactions on Systems, Man, and Cybernetics: Systems*, [25]vol. 50(12), pp. 4905-4918. doi: 10.1109/TSMC.2018.2884510, 2020.

[26] X. Liu, S. Wang, S. Lu, Z. Yin, X. Li, L. Yin, and W. Zheng Adapting Feature Selection Algorithms for the Classification of Chinese Texts *Systems*, vol. 11(9), pp. 483. doi: 10.3390/systems11090483, 2023.

[27] C. Zhang, L. Zhou, and Y. Li Pareto Optimal Reconfiguration Planning and Distributed Parallel Motion Control of Mobile Modular Robots *IEEE Transactions on Industrial Electronics*, doi: 10.1109/TIE.2023.3321997, 2023.

[28] X. Yang, X. Wang, S. Wang, K. Wang, and M. B. Sial Finite-time adaptive dynamic surface synchronization control for dual-motor servo systems with backlash and time-varying uncertainties *ISA Transactions*, vol. 137, pp. 248-262. doi: https://doi.org/10.1016/j.isatra.2022.12.013, 2023

[29] Y. Zhang, S. Li, S. Wang, X. Wang, and H. Duan Distributed bearing-based formation maneuver control of fixed-wing UAVs by finite-time orientation estimation *Aerospace Science and Technology*, vol. 136, pp. 108241. doi: https://doi.org/10.1016/j.ast.2023.108241, 2023.

[30] M. Shi, W. Hu, M. Li, J. Zhang, X. Song, and W. Sun Ensemble regression based on polynomial regression-based decision tree and its application in the in-situ data of tunnel boring machine *Mechanical Systems and Signal Processing*, vol. 188, pp. 110022. doi: https://doi.org/10.1016/j.ymssp.2022.110022, 2023.

[31] X. Liu, T. Shi, G. Zhou, M. Liu, Z. Yin, L. Yin, and W. Zheng Emotion classification for short texts: an improved multi-label method *Humanities and Social Sciences Communications*, vol. 10(1), 306. doi: 10.1057/s41599-023-01816-6, 2023.

[32] X. Zhang, , Y. Shen, X. Yuan, and Z. Lu, Hierarchical Velocity Optimization for Connected Automated Vehicles With Cellular Vehicle-to-Everything Communication at Continuous Signalized Intersections *IEEE Transactions on Intelligent Transportation Systems*, doi: 10.1109/TITS.2023.3274580, 2023.

[33] B. Cheng, D. Zhu, and J. Chen Situation-Aware IoT Service Coordination Using the Event-Driven SOA Paradigm *IEEE Transactions on Network and Service Management*, vol. 13(2), pp. 349-361. doi: 10.1109/TNSM.2016.2541171, 2016.

[34] S. Lu, M. Liu, L. Yin, Z. Yin, and X. Kong The multi-modal fusion in visual question answering: a review of attention mechanisms*PeerJ Computer Science*, vol. 9, e1400. doi: 10.7717/peerj-cs.1400, 2023.

[35] K. Zhao, Z. Jia, F. Jia, and H. Shao Multi-scale integrated deep self-attention network for predicting remaining useful life of aero-engine *Engineering Applications of Artificial Intelligence*, 120, 105860. doi: https://doi.org/10.1016/j.engappai.2023.105860, 2023.

[36] J. Hu, Y. Wu, and B. K. Ghosh Consensus Control of General Linear Multiagent Systems With Antagonistic Interactions and Communication Noises *IEEE Transactions on Automatic Control*, vol. 64(5), pp. 2122-2127. doi: 10.1109/TAC.2018.2872197, 2019.

[37] B. Chen, J. Hu, Y. Wu, and B. K. Ghosh Finite-Time Velocity-Free Rendezvous Control of Multiple AUV Systems With Intermittent Communication *IEEE Transactions on Systems, Man, and Cybernetics: Systems*, vol. 52(10), pp. 6618-6629. doi: 10.1109/TSMC.2022.3148295, 2022.

[38] D. Zhou, M. Sheng, J. Li, and Z. Han Aerospace Integrated Networks Innovation for Empowering 6G: A Survey and Future Challenges *IEEE Communications Surveys & Tutorials*, vol. 25(2), pp. 975-1019. doi: 10.1109/COMST.2023.3245614, 2023.

[39] C. Zhang The active rotary inertia driver system for flutter vibration control of bridges and various promising applications *Science China Technological Sciences*, doi: 10.1007/s11431-022-2228-0, 2022.

[40] Q. Meng, Q. Ma, and Y. Sh, Adaptive Fixed-Time Stabilization for a Class of Uncertain Nonlinear Systems, *IEEE Transactions on Automatic Control*, Vol. 68(11), 6929–6939, 2023.

[41] J. Zhang, Y. Liu, Z. Li, and Y. Lu Forecast-Assisted Service Function Chain Dynamic Deployment for SDN/NFV-Enabled Cloud Management Systems *IEEE Systems Journal*, doi: 10.1109/JSYST.2023.3263865, 2023.

[42] A. She, L. Wang, Y. Peng, and J. Li Structural reliability analysis based on improved wolf pack algorithm AK-SS *Structures*, [42]vol. 57, pp. 105289. doi: https://doi.org/10.1016/j.istruc.2023.105289, 2023.

[43] Q. Gu, S. Li, and Z. Liao Solving nonlinear equation systems based on evolutionary multitasking with neighborhood-based speciation differential evolution *Expert Systems with Applications*, vol. 238, pp. 122025. doi: https://doi.org/10.1016/j.eswa.2023.122025, 2024.

[44] J. Mou, K. Gao, P. Duan, J. Li, A. Garg, and R. Sharma A Machine Learning Approach for Energy-Efficient Intelligent Transportation Scheduling Problem in a Real-World Dynamic Circumstances *IEEE Transactions on Intelligent Transportation Systems*, doi: 10.1109/TITS.2022.3183215, 2022.

[45] S. Li, H. Chen, H. Chen, Y. Xiong, and Z. Song Hybrid Method with Parallel-Factor Theory, a Support Vector Machine, and Particle Filter Optimization for Intelligent Machinery Failure Identification *Machines*, vol. 11(8), pp. 837. doi: 10.3390/machines11080837, 2023

[46] B. Cao, Z. Sun, J. Zhang, and Y. Gu Resource Allocation in 5G IoV Architecture Based on SDN and Fog-Cloud Computing *IEEE transactions on intelligent transportation systems*, vol. 22(6), pp. 3832-3840. doi: 10.1109/TITS.2020.3048844, 2021.

[47] Q. Zhong, S. Han, K. Shi, S. Zhong, and O. Kwon Co-Design of Adaptive Memory Event-Triggered Mechanism and Aperiodic Intermittent Controller for Nonlinear Networked Control Systems *IEEE Transactions on Circuits and Systems II: Express Briefs,* vol. 69(12), pp. 4979-4983. doi: 10.1109/TCSII.2022.3188036, 2022.

[48] B. Cao, J. Zhao, Y. Gu, and P. Yang Security-Aware Industrial Wireless Sensor Network Deployment Optimization *"IEEE Transactions on Industrial Informatics*, vol. 16(8), pp. 5309-5316. doi: 10.1109/TII.2019.2961340, 2020

[49] B. Cao, J. Zhao, Y. Gu, and X. Ma Applying graph-based differential grouping for multiobjective large-scale optimization *Swarm and Evolutionary Computation*, 53, 100626. doi: https://doi.org/10.1016/j.swevo.2019.100626, 2020.

[50] J. Liu, C. Fan, Y. Peng, J. Du, Z. Wang, and C. Chu Emergent Leader-follower Relationship in Networked Multiagent Systems *SCIENCE CHINA Information Sciences*, doi: https://doi.org/10.1007/s11432-022-3741-3, 2023.

[51] Z. Xuemin, R. Ying, X. Zenggang, D. Haitao, X. Fang, and L. Yuan Resource-Constrained and Socially Selfish-Based Incentive Algorithm for Socially Aware Networks *Journal of Signal Processing Systems*, doi: 10.1007/s11265-023-01896-2, 2023.

[52] Q. Wu, J. Fang, and F. Luo Monte Carlo Simulation-Based Robust Workflow Scheduling for Spot Instances in Cloud Environments *Tsinghua Science and Technology*, vol. 29(1), pp. 112-126. doi: 10.26599/TST.2022.9010065, 2024

[53] J. Chen, Q. Wang, H. H. Cheng, W. Peng, and W. Xu A Review of Vision-Based Traffic Semantic Understanding in ITSs *IIEEE Transactions on Intelligent Transportation Systems*, vol. 23(11), pp. 19954-19979. doi: 10.1109/TITS.2022.3182410, 2022

[54] K. Li, L.Ji, S. Yang, H. Li, and X. Liao. Couple-Group Consensus of Cooperative–Competitive Heterogeneous Multiagent Systems: A Fully Distributed Event-Triggered and Pinning Control Method *IEEE Transactions on Cybernetics*, vol. 52(6), pp. 4907-4915. doi: 10.1109/TCYB.2020.3024551, 2022

[55] X. Ma, Z. Dong, W. Quan, Y. Dong, and Y. Tan Real-time assessment of asphalt pavement moduli and traffic loads using monitoring data from Built-in Sensors: Optimal sensor placement and identification algorithm *Mechanical Systems and Signal Processing*, vol. 187, pp. 109930, doi: https://doi.org/10.1016/j.ymssp.2022.109930, 2023.

Journal's webpage: http://univagora.ro/jour/index.php/ijccc/

This journal is a member of, and subscribes to the principles of,
the Committee on Publication Ethics (COPE).
https://publicationethics.org/members/international-journal-computers-communications-and-control

Cite this paper as:

Chen Zy; Meng, Y.; Wang, R.-Y.; Chen, T.(2024). Neural ordinary differential grey algorithm to forecasting MEVW systems, *International Journal of Computers Communications & Control*, 19(1), 4676, 2024.

https://doi.org/10.15837/ijccc.2024.1.4676